cance here is[23]

$$C=\tfrac{3}{4}C_{44}+\tfrac{1}{5}(C_{11}-C_{12}).$$

We note a good agreement between the experimental values and those calculated from Keyes's model. The activation volume for migration of positive-ion vacancies in LiBr is smaller than that in either NaCl or KCl, as expected because of the comparatively smaller atomic volume of lithium.

It is noted from Table IV that V_m in ionic crystals is greater than the atomic volume available for the cation in the crystal lattice. Also, the results of the present experiments on LiBr and those of Kurnick on AgBr show clearly that V_f and V_t $(=V_f+V_m)$ are larger than the molar volume. On the other hand, the experiments of Hultsch and Barnes[9] and others[24] on metals indicate that volumes for self-diffusion (V_f+V_m) are considerably smaller than the atomic volumes. Aluminum is the only metal which seems to be an exception.[4] In metals such as copper considerable inward relaxation may occur about a vacancy as has been shown by Tewordt.[25] Pierce[23] observes that the large size of V_f in ionic crystals arises because the nearest neighbors of a given ion are repelled once it is removed from the original lattice site to form a vacancy. These Coulomb repulsions of ions are also probably responsible for the observation of large V_m in these crystals.

[23] C. B. Pierce, Phys. Rev. **123**, 744 (1961).
[24] D. Lazarus, in *Solids Under Pressure*, edited by W. Paul and D. M. Warschauer (McGraw-Hill Book Co., New York, 1963).

ACKNOWLEDGMENTS

The authors are grateful to Dr. G. W. Stupian for assistance in NMR experiments and for many suggestions. Thanks are due to Dr. P. G. McCormick for assistance in high-pressure experiments. Helpful discussions with Professor R. M. Cotts and efforts of G. E. Schmidt in growing the single crystals of LiBr are acknowledged.

[25] L. Tewordt, Phys. Rev. **99**, 61 (1958).

PHYSICAL REVIEW B VOLUME 1, NUMBER 1 1 JANUARY 1970

Charge-Transfer Spectra of Transition-Metal Ions in Corundum†

H. H. TIPPINS
Aerospace Corporation, El Segundo, California 90245
(Received 17 July 1969)

The ultraviolet absorption spectrum of corundum (Al_2O_3) containing dilute concentrations of the 3*d*-series transition-metal ions Ti^{3+}, V^{3+}, Cr^{3+}, Mn^{4+}, Fe^{3+}, and Ni^{3+} was measured at room temperature and at liquid-nitrogen temperature for photon energies in the range 3–9 eV. The most important features of the observed spectra are (a) the peak positions are characteristic of the particular impurity ion; (b) the peak positions and widths (~0.7 eV) are independent of temperature over the range studied; and (c) the integrated intensities are strong. The spectra are identified with the allowed transition whereby an electron is transferred from a nonbonding orbital, localized predominantly on the $O^{=}$ ligands, to either the $t_{2g}(\pi^*)$ or $e_g(\sigma^*)$ antibonding orbital, localized predominantly on the metal ion. The position in energy of the first absorption peak for the various ions of the series relative to one another and to the position of the intrinsic absorption edge of Al_2O_3 is in good agreement with the charge-transfer model.

I. INTRODUCTION

THE optical spectra of transition-group metal ions, present as substitutional impurities in ionic crystals, have been the subject of intense investigation in recent years.[1,2] These investigations have attempted to obtain a fundamental understanding of the varied colors and luminescent properties exhibited by the ions in different crystalline environments, and considerable progress has been made. However, with very few exceptions, the studies have been confined to spectra that arise as a result of transitions between energy levels internal to the substituted metal ion. These energy levels are those of the free ion modified by the intense crystalline electric fields of the host lattice. The present paper treats spectra that arise as a result of transitions between initial electronic states of the host crystal to final electronic states of the substitutional metal ion.

The absorption spectrum of a typical 3*d*-series ion at a concentration of about 10^{-2} mole % in Al_2O_3 shows several moderately strong absorption bands extending from the near infrared (IR) to the near uv, and then an abrupt intense cutoff at several eV on the low-energy side of the fundamental absorption edge of the host lattice (approximately 9 eV for Al_2O_3). The lower-energy transitions are the parity-forbidden transitions internal to the substituted ion, which have an oscillator strength

† This work was supported by the U. S. Air Force under Contract No. F04701-68-C-0200.
[1] D. S. McClure, Solid State Phys. **9**, 399 (1959).
[2] C. J. Ballhausen, *Introduction to Ligand Field Theory* (McGraw-Hill Book Co., New York, 1962).

of about 10^{-4}, while the intense cutoff at higher energies is a result of the charge-transfer process, which is fully allowed.

The spectra of the internal transitions of $3d$-series ions in Al_2O_3 have been studied in great detail for all ions of the series by many workers and were reviewed by McClure.[3] The objectives of the present study were to (a) extend the previous spectral measurements for the $3d$ series down to the wavelength of the intrinsic cutoff, (b) relate these spectra to those of the $3d$-series internal transitions and the intrinsic Al_2O_3 absorption, (c) determine the systematics of the charge-transfer threshold as a function of the substituted metal ion, and (d) determine if a simple charge-transfer model could provide an adequate interpretation of the short-wavelength spectra. The original intent has been largely successful and the simple charge-transfer picture was found to be surprisingly effective for the interpretation of the short-wavelength spectra.

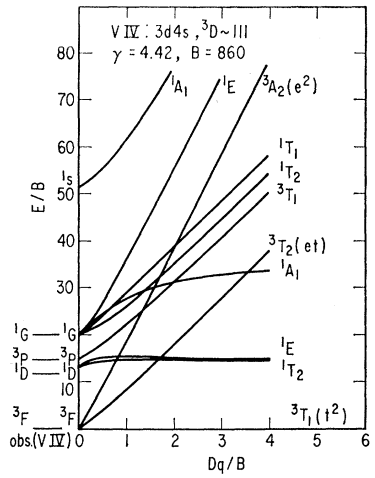

FIG. 1. Splitting of the free-ion energy levels of the electron configuration d^2 due to a crystalline electric field having octahedral symmetry. E is the energy, and Dq and B are parameters that represent, respectively, the strength of the crystal field and Coulomb interaction between electrons (Ref. 6).

II. THEORY

Ions of the first transition or iron-group series have an incomplete shell of $3d$ electrons as their outermost electrons. Extensive optical and electron paramagnetic resonance (EPR) spectroscopy[3,4] has established that, in solid solution, these ions enter substitutionally for the host Al^{3+} ion. The Al_2O_3 crystal structure is fairly complicated,[5] but for the purpose of this report the most important aspect of the structure is that the local environment of the Al^{3+} site is that of a slightly distorted octahedral array of six oxygen ions. As a good first approximation, the distortion of the octahedron may be neglected, as can the effects of all ions more distant than the six nearest neighbors. The intense electrostatic field of the $O^=$ ions partially removes the fivefold degeneracy that exists for a single d electron in the free ion and produces an energy separation designated 10 Dq, which is typically a few eV. The states of the lower and upper energy levels belong, respectively, to the triply degenerate t_{2g} and doubly degenerate e_g representations of the cubic group O_h.

The magnitude of the splitting produced by the crystalline electric field is, in general, comparable to the Coulomb interaction between the $3d$ electrons. These two interactions must, therefore, be treated simultaneously in the perturbation description of ions with more than one d electron. A complete analysis of the splitting of the free-ion energy levels due to a static crystalline field having cubic symmetry has been performed by Tanabe and Sugano[6] for all ions of the $3d^n$ series. This would be the situation, for example, for a transition-metal ion surrounded by $O^=$ ions fixed at the vertices of an octahedron. Although much more sophisticated and accurate treatments[7] are now available, the results of Tanabe and Sugano are still extremely valuable because of the simplicity of the model. Figure 1 shows the result of their calculation for V^{3+}, which has the electron configuration d^2. The energy E is plotted versus the strength of the crystalline field Dq. Both E and Dq are normalized to the Racah parameter B, which is essentially a measure of the Coulomb interaction between electrons. In terms of the standard radial integrals F_2 and F_4, $B=F_2-5F_4$. The observed free-ion levels of V^{3+} are shown at the left of the diagram. The crystal-field-split levels are labeled by their octahedral group representations, and the spin superscripts have the same meanings as for the free ion. The lowest level is kept horizontal on the diagram. Spin-orbit coupling of the d electrons is comparable in magnitude ($\sim 10^{-2}$ eV) to the effect of departure of the crystalline field from cubic symmetry. These two effects are included as further perturbations to the states and energies derived from the combined cubic-crystal field and Coulomb-interaction calculation, and are necessary to interpret the optical fine structure and EPR results. However, these terms are not pertinent to the present work and, therefore, will not be considered further.

Transition intensities between these energy levels are weak because they are d-to-d and hence violate the Laporte selection rule, which requires that the parities of the initial and final states be different. If, in addition, $\Delta S \neq 0$ for a transition, an even stronger selection rule operates. The Laporte selection rule is relaxed by the presence of odd components of the static crystal field (arising from the slight static distortion of the $O^=$

[3] D. S. McClure, J. Chem. Phys. **36**, 2757 (1962).
[4] S. Geschwind and J. P. Remeika, J. Appl. Phys. Suppl. **33**, 370 (1962).
[5] R. E. Newnham and Y. M. DeHaan, Z. Krist. **117**, 235 (1962).
[6] Y. Tanabe and S. Sugano, J. Phys. Soc. Japan **9**, 753 (1954).
[7] J. Owen and J. H. M. Thornley, Rept. Progr. Phys. **29**, 675 (1966).

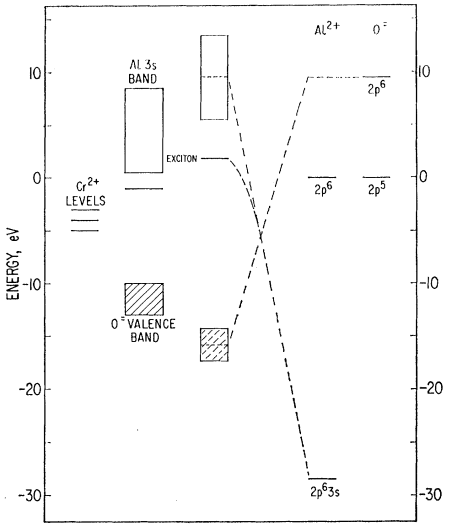

FIG. 2. Energy-level diagram for Al_2O_3. The displacement of the free-ion energy levels (shown at the right) when the lattice is formed is indicated by the dashed lines. The energy diagram as it seems to exist experimentally is shown to the left of center, and the approximate position of a typical $3d$-series ion (empty Cr^{2+} levels) relative to the band gap is shown at the left.

octahedron), and, in addition, odd components of the lattice vibrations. These mechanisms result in an oscillator strength of about 10^{-4}. The spin selection rule is relaxed by spin-orbit interaction.

The energy required for a charge-transfer process is determined by considering the transfer of an electron from one oxygen ion to a nearest-neighbor cation (M^{3+})

$$O^=(2p^6)+M^{3+}(3d^n) \rightarrow O^-(2p^5)+M^{2+}(3d^{n+1}). \quad (1)$$

The threshold energy for this process can be written in the form

$$h\nu_T=\epsilon_+ +\epsilon_- -e^2/r_0+\chi(O^=)-I(M^{2+})-\psi_{pol}+\Delta E_d, \quad (2)$$

where ϵ_+ and ϵ_- are the magnitudes of the electrostatic lattice energies at the metal ion and $O^=$ sites (i.e., the Madelung energy), r_0 is the separation between the two ions, e is the electronic charge, and e^2/r_0 represents the electron-hole binding energy of the separated charge. χ is the oxygen electron affinity, I is the ionization potential of the divalent metal ion, ψ_{pol} is the polarization energy of the dipole formed by the charge transfer, and ΔE_d is a term added to take account of the difference of the d-electron stabilization energy for the two different configurations of the divalent and trivalent ions. This expression is derived[8,9] by considering a sequence of operations involving removal of the ions from the crystal, transfer of the electron between free ions, and then returning the ions to their original position in the crystal. Although an accurate evaluation of the various terms in Eq. (2) is extremely difficult, this equation affords considerable insight into the systematics of the threshold for the charge-transfer process for the various ions of the $3d$ series.

Consider Eq. (2) as it applies to the intrinsic absorption of Al_2O_3. This absorption also arises from a similar type of charge-transfer process except that the final state resides on the host Al^{3+} ion:

$$O^=(2p^6)+Al^{3+}(2p^6) \rightarrow O^-(2p^5)+Al^{2+}(2p^63s). \quad (3)$$

In Fig. 2 the free-ion energy levels of $O^=$ and Al^{2+} are shown to the right. It should be noted that for widely separated free ions it is energetically more favorable for the second electron of $O^=$ to be on the Al ion to form Al^{2+}, instead of on the $O^=$ ion. In the crystal, however, the electron can achieve a lower energy by being on $O^=$ and leaving the Al^{2+} $3s$ level empty, i.e., Al^{3+}, because of the energy reduction afforded by the ionic electrostatic energy. Thus the $O^=$ $2p$ level and Al^{2+} $3s$ level are shifted relative to one another, as indicated by the dashed lines, to the positions shown in the center of Fig. 2, and in addition these levels are broadened into bands in the crystal. For transfer between neighboring ions, the additional term $-e^2/r_0$ is included to account for the exciton binding energy, which further reduces the energy threshold. The term ΔE_d is zero for the intrinsic process, since there are no d electrons on Al^{3+}. The relative positions of the top of the oxygen valence band and the first exciton were calculated from the known Al_2O_3 Madelung energy, and r_0, χ, and I, and are, therefore, as shown in the center of Fig. 2. The only term of Eq. (2) not included is ψ_{pol}, which should perhaps reduce the separation by another few eV.[8] The situation, as it seems to exist experimentally, is shown just to the left of center in Fig. 2, and while the agreement is not perfect it is as good as might be expected for such a semiclassical calculation of the absolute energy separation.

Now consider the effect of having a cation different from Al^{3+} for the final state. If the ion has approximately the same ionic radius as Al^{3+}, so that lattice distortion effects can be neglected, then only the terms $-I(M^{2+})$ and ΔE_d should be characteristic of the metal ion; all others should be independent of the particular metal ion as a first approximation. Equation (2) may, therefore, be rewritten

$$h\nu_T=C-I(M^{2+})+\Delta E_d, \quad (4)$$

where C is a constant energy common to all ions of the series. Note especially that the third ionization energy $I(M^{2+})$ of the transition-metal ion occurs with a minus sign so that ions having $I(M^{2+})>I(Al^{2+})$ should have transitions on the low-energy side of the intrinsic absorption. This is true[10] for all $3d$-series ions

[8] N. F. Mott and R. W. Gurney, *Electronic Processes in Ionic Crystals* (Oxford University Press, London, 1948), p. 95.
[9] F. Seitz, *The Modern Theory of Solids* (McGraw-Hill Book Co., New York, 1940), Ch. 12.
[10] C. E. Moore, *Atomic Energy Levels* (U. S. Government Printing Office, National Bureau of Standards, Washington, D. C., 1958), Circular 467, Vol. III, p. XXXIV.

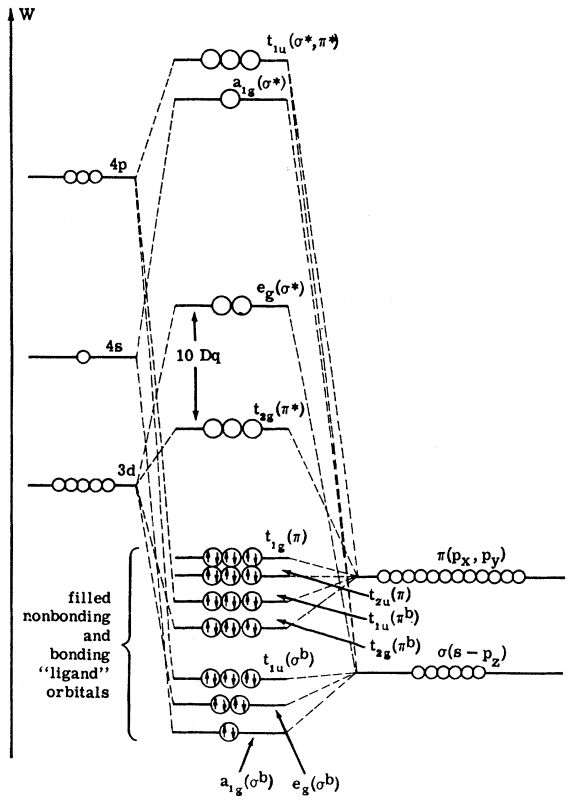

FIG. 3. Molecular orbital energy-level diagram for an octahedral complex after the work of Ballhausen and Gray (Ref. 12). The metal-ion energy levels at the left interact with the ligand orbitals at the right to form the molecular orbitals shown in the center. Parity-allowed charge-transfer transitions can occur from either the $t_{2u}(\pi)$ or $t_{1u}(\pi)$ levels to empty $t_{2g}(\pi^*)$ or $e_g(\sigma^*)$ levels.

except Ti, and even in this case the crystal-field stabilization energy is apparently sufficient to situate the Ti charge-transfer absorption below the intrinsic absorption. As an example, the approximate positions of the empty Cr^{2+} energy levels within the Al_2O_3 band gap are shown at the left in Fig. 2. Equation (4), therefore, gives a basis for comparison of the energy threshold for the various ions of the series.

The discussion has so far neglected the effects of covalent bonding[2,7,11,12] between the oxygen and metal ions. This aspect of the problem is very important in the interpretation of the charge-transfer spectra. It is even more important for the transition ions than it is for the aluminum ion for two reasons; first, the transition-ion energy levels are closer to the oxygen levels, and second, the $3d$ wave functions are larger and have greater overlap with the oxygen wave function. Figure 3 shows the bonding scheme for an octahedral complex after the work of Ballhausen and Gray.[12] The metal-ion energy levels at the left interact with the ligand orbitals of the same symmetry types at the right to form the molecular orbital energy levels of the complex, as shown in the center. For example, the e_g part of the d-electron manifold interacts with the E_g component of the σ-bonded ligand p functions, whereas the t_{2g} part of the d-electron manifold is bonded with the T_{2g} component of the π-bonded ligand p functions, etc. Only the high-energy f and g orbitals of the metal ion have representations containing T_{1g} and T_{2u}. The $t_{1g}(\pi)$ and $t_{2u}(\pi)$ ligand orbitals can, therefore, be considered nonbonding for all practical purposes and, consequently, are probably the highest in energy of the ligand orbitals. From the molecular orbital standpoint, the crystal-field splitting 10 Dq between the antibonding $t_{2g}(\pi^*)$ and $e_g(\sigma^*)$ orbitals, located predominantly on the metal ion, arises as a result of the greater strength of the σ bonds, owing to greater overlap of the σ wave functions. The more complete model of the charge-transfer process, which takes into account the covalent bonding, therefore envisions the excitation of an electron from one of the higher-lying bonding or nonbonding odd-parity states, e.g., $t_{1u}(\pi)$ or $t_{2u}(\pi)$, to the even-parity antibonding metal-ion states $t_{2g}(\pi^*)$ or $e_g(\sigma^*)$. The oxygen states are broadened into bands that may overlap one another enough to form one $O^=$ valence band, as pictured in Fig. 2.[9] An important aspect of the molecular orbital description of the states is that the hole left behind on the oxygen system is distributed over more than one of the $O^=$ neighbors of the metal ion to which the transition occurs. For example, one of the $t_{2u}(\pi)$ nonbonding orbitals is shown in Fig. 4, and this would, therefore, represent the hole if the excitation occurred from the $t_{2u}(\pi)$ state, the probable initial state of the transition.

This section has briefly described the theoretical aspects of the relationship that exists between earlier crystal field theory, covalent bonding, internal d-to-d transitions, intrinsic host absorption, and the process of charge transfer to the substituted $3d$ ion. Detailed

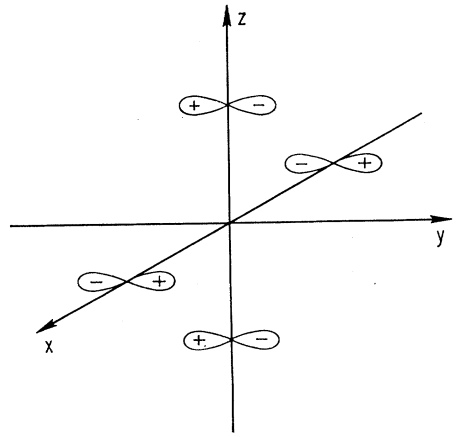

FIG. 4. Electron distribution for the $t_{2u}(\pi)$ nonbonding molecular orbital. This is believed to be the state from which the threshold charge-transfer originates, so that the above figure represents the "hole" left on the ligand system after the transfer.

[11] L. E. Orgel, *An Introduction to Transition-Metal Chemistry Ligand-Field Theory* (Methuen and Co., Ltd., London, 1960).
[12] C. J. Ballhausen and H. B. Gray, *Molecular Orbital Theory* (W. A. Benjamin, Inc., New York, 1964).

calculations of the absolute energy positions of the charge-transfer bands in Al_2O_3 were not attempted in the present study. Solution of the molecular orbital problem of the free MO_6 complex for all the $3d$-series ions would require considerable labor and probably would still not provide a completely satisfactory quantitative description of the experimental results. A complete description must take account of the additional complications that arise because the MO_6 complexes are embedded in a crystal lattice.

To summarize the present model, the experimental results described below are interpreted as arising from allowed electronic transitions between molecular orbital states of the host oxygen ions and final states on the substitutional metal ion. The oxygen levels form a band because of their wave function overlap, whereas the transition-metal ion levels are relatively sharp because of their low concentration and consequent small wave function overlap. The absorption thresholds for the various ions of the series should be related to their third ionization potential and crystal-field stabilization energy by Eq. (4).

III. EXPERIMENTAL DETAILS

Thin dilute samples are required for the study of charge-transfer spectra because of the large optical density that arises from the allowed nature of the transition. The peak absorption coefficient for a transition of oscillator strength f and half-width $\Delta\tilde{\nu}$ cm^{-1} is

$$K_m = 0.56\times10^{-12}(Nf/\Delta\tilde{\nu})\ cm^{-1}, \quad (5)$$

where N is the number of absorbers per cm^3. For an Al_2O_3 crystal 1 mm thick, containing 0.01 mole% absorbers having $f\sim0.2$ and $\Delta\tilde{\nu}\sim5000$ cm^{-1}, the optical density $D\sim5$, where D is defined from

$$D=\log_{10}(I_0/I)=\log_{10}e^{Kx}. \quad (6)$$

Here I_0 and I are the light intensities incident on and transmitted by a sample of thickness x, K is the absorption coefficient, and the second equality neglects reflections. The practical range of measurement of D is approximately 0 to 3 because of limitations imposed by scattered light. Therefore, for transitions that are nearly fully allowed, the maximum measurable optical density is exceeded for quite low concentrations of impurities.[13] The optimum combination of metal-ion concentration and sample thickness was determined by trial and error for each of the samples. It is important that the metal-ion concentration exceed, by a substantial margin, the concentration of other impurities that produce absorptions in the same energy range. On the other hand, the samples must be dilute enough that their required thickness is not less than about 50 μ, since thinner samples are too fragile.

Both Verneuil-grown and oxide-flux-grown single crystals were used for these measurements. The Verneuil-grown material was obtained from the Linde Co., except for the Ni^{3+}-doped material, which was obtained from Semi-Elements, Inc. The samples were fabricated from slices sawed from the boule and then lapped and polished with fine diamond grit on a high-speed lap. No attempt was made to orient these samples. The flux-grown samples were grown by Chase[14] from PbF_2-Bi_2O_3 melts. The growth habit from this system is such that the single crystals are thin platelets with the c axis normal to the plate. Typical thickness is a few tenths of a millimeter, with a cross section ranging from 0.1–1 cm^2. These crystals were used as-grown by careful selection of the samples for quality and thickness. A semiquantitative spectrographic analysis was performed on all the samples to verify that they indeed contained the ion specified and also to reveal the presence of unwanted impurities that might affect the absorption spectrum in the region of interest. These analyses have been found to be reliable to within a factor of 2 for controlled samples analyzed previously.

The absorption spectra were measured for each sample both at room temperature and, by use of a cold-finger Dewar, at liquid-nitrogen temperature. The spectra were found to be virtually identical at the two temperatures. The difference was so insignificant that only the room-temperature spectra are shown in the curves to follow. The spectral range 3–6 eV was covered by use of a Cary Model 14 recording spectrophotometer, which directly records the optical density as a function of wavelength with a resolution better than 1 Å in this range. For the range 6–9 eV, a 1-m Jarrell-Ash–Seya-Namioka-type vacuum uv monochromator was used. A hydrogen discharge tube was used for the source, and an EMI 6256S photomultiplier tube was used to detect the fluorescence from sodium salicylate. The optical density was computed point-by-point by comparison of the light incident on and transmitted by the sample. The range of operation for the two instruments overlapped by about 1 eV, and the agreement between the results obtained was excellent in the overlap region. The spectra were also found to be reproducible both on different runs of the same sample and on different samples cut from the same boule or grown from the same flux melt.

IV. RESULTS

Figures 5–10 show the charge-transfer spectra of the various $3d^n$ ions. The sample thickness t is given in each case. Note that for some samples, t is only a few thousandths of an inch, yet the absorption peaks are

[13] This makes intrinsic absorption measurements on wide band-gap materials very difficult, since the presence of impurities having transitions at longer wavelengths than the intrinsic band edge makes the crystal opaque before the edge is reached and hence obscures its wavelength location.

[14] A. B. Chase, J. Am. Ceram. Soc. 49, 233 (1966).

very intense. The spectra have not been corrected for reflections.

The spectrum of V^{3+} is shown in Fig. 5. This ion is shown first because its spectrum affords a particularly good experimental comparison of the internal transitions with the charge-transfer transitions. The weaker low-energy peaks at 3.1 and 3.9 eV were studied by several workers and were successfully identified with internal transitions of V^{3+}.[3,15] These are spin-allowed crystal-field transitions from the $^3T_1(t_{2g}^2)$ ground state to the $^3T_1(t_{2g}e_g)$ and $^3A_2(e_g^2)$ excited states, respectively (c.f. Fig. 1). The intense peak at 5.75 eV is identified with the charge-transfer transition. Since V^{3+} has one unfilled t_{2g} orbital, the final state of the one-electron transition should be this orbital, so that the configuration t_{2g}^3 is formed. Note that a sample much thicker or more concentrated (by approximately a factor of 5) would be required to enhance the internal transitions to their optimum intensity. On the other hand, if this sample were even twice as thick, or twice the concentration, the charge-transfer peak would be completely obscured because it would exceed the practical maximum range of measurement of an optical density of 3.0. Therefore, the thickness and concentration required are such that samples for the two types of measurements are mutually exclusive. An estimate was made of the oscillator strength associated with the 5.75-eV absorption peak. The result of 0.05 is probably correct only to about a factor of 2, mainly because of the inaccuracy of the spectrochemical analysis.

Figure 6 shows the spectrum of Ti^{3+}. A broad absorption centered near 6.9 eV is observed to blend into the intrinsic absorption edge. The considerably larger breadth of the Ti^{3+} absorption as compared to the breadth of the other ions is consistent with the expected broadening mechanism and is discussed in greater detail below. The hump near 4.8 eV is probably the charge transfer of some trace impurity, most likely Fe^{3+}, since this crystal did contain traces of Fe and the energy position is consistent (see the discussion of the Fe^{3+} spectrum below). This structure presumably does not arise from an internal Ti^{3+} transition, since Ti^{3+} has the electron configuration t_{2g}^1 and therefore the only possible crystal-field transition is $t_{2g} \rightarrow e_g$, which occurs as a diffuse peak near 2.5 eV.[3] The charge-transfer transition should result in the final state t_{2g}^2 of the Ti^{2+} ion.

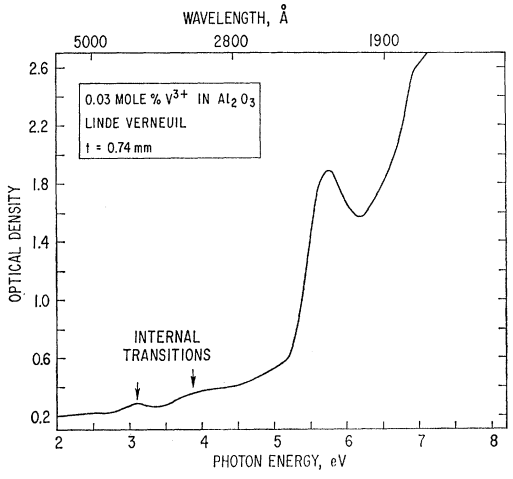

FIG. 5. Absorption spectrum of V^{3+} in Al_2O_3. The intense peak at 5.75 eV is the charge-transfer threshold.

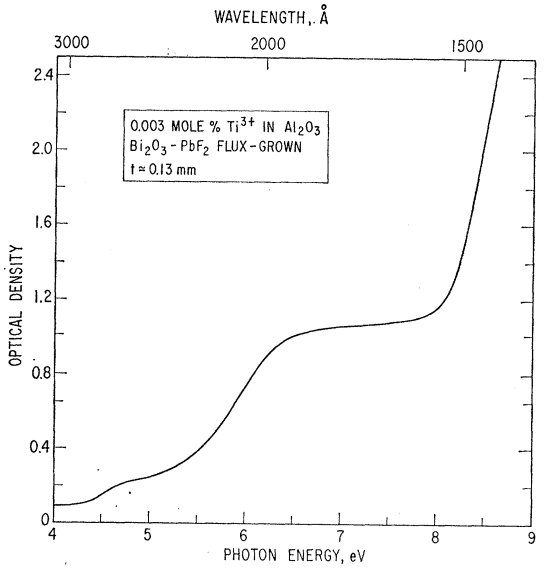

FIG. 6. Absorption spectrum of Ti^{3+} in Al_2O_3. The broad shoulder near 7 eV is identified with the charge-transfer transition.

The charge-transfer spectrum of 0.01% Cr^{3+} in Al_2O_3 (Fig. 7) shows a single well-resolved peak at 6.9 eV. Ruby has been studied extensively by many workers throughout the entire spectral range; Loh[16] has reported an absorption peak at 7 eV, and Lemonnier *et al.*[17] report structure on a rising edge in this region. Since the electron configuration of the Cr^{3+} ion prior to a charge-transfer transition is t_{2g}^3 (all spins parallel), the added electron must enter an unfilled e_g orbital to form $t_{2g}^3e_g$. This requires additional energy amounting to 10 Dq over that required for transfer to t_{2g}. For example, compare the peak position of $Cr^{3+}(t_{2g}^3)$ with that of $V^{3+}(t_{2g}^2)$. The Cr^{2+} ionization potential is larger than that of V^{2+} by 1.6 eV. This should place the Cr^{3+} peak at lower energy than that of V^{3+} [cf. Eq. (4)], were it not for the effect of the crystal-field term, which is sufficient to shift the Cr^{3+} peak over to the high-energy side of V^{3+}.

Figure 8 shows the spectra of two different samples containing Mn^{4+}, charge-compensated with Mg^{2+}. The fact that the active ion in this case is not trivalent and

[15] M. H. L. Pryce and W. A. Runciman, Discussions Faraday Soc. **26**, 34 (1958).

[16] E. Loh, J. Chem. Phys. **44**, 1940 (1966).

[17] J. Lemonnier, M. Priol, and S. Robin, Compt. Rend. **257**, 1608 (1963).

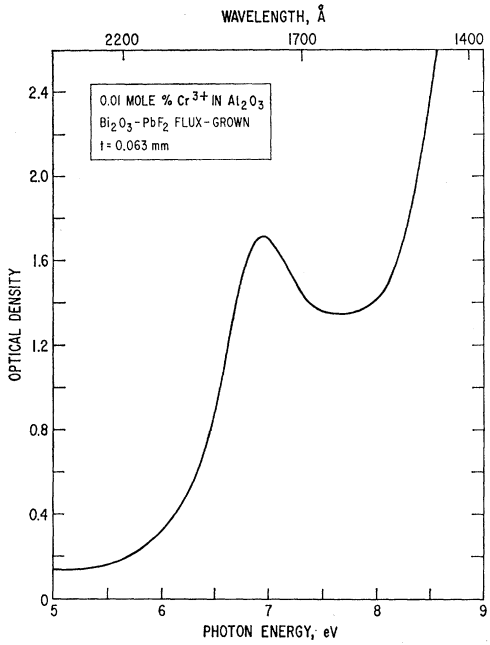

FIG. 7. Absorption spectrum of Cr^{3+} in Al_2O_3 (ruby). An intense charge-transfer peak is observed at 6.94 eV.

that a charge compensator is present complicates the interpretation. However, the spectra are fairly well resolved and the peaks are undoubtedly due to charge transfer to Mn^{4+} and so are included for completeness, although there was no attempt to make a quantitative interpretation of the peak positions in terms of the charge-transfer model. The weak bump near 2.6 eV for the flux-grown sample is the internal $^4A_2 \rightarrow {}^4T_2$ absorption reported by Geschwind *et al.*,[18] who also reported a steeply rising edge beginning at 3.5 eV. Note that the large concentration difference in the two

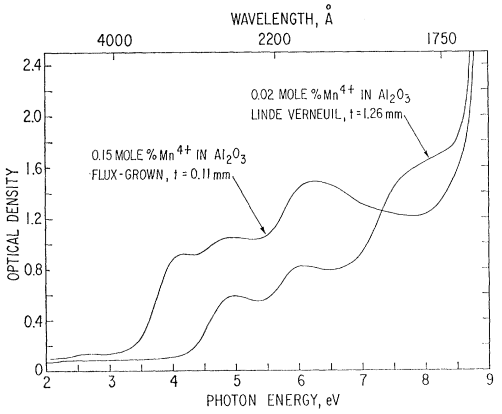

FIG. 8. Absorption spectrum of two different samples of Mn^{4+} in Al_2O_3. All bands, except the very weak ones between 2 and 3 eV, are due to charge transfer. The peak near 4.1 eV for the flux-grown sample is believed to be the Mn^{3+} charge-transfer threshold.

[18] S. Geschwind *et al.*, Phys. Rev. **126**, 1684 (1962).

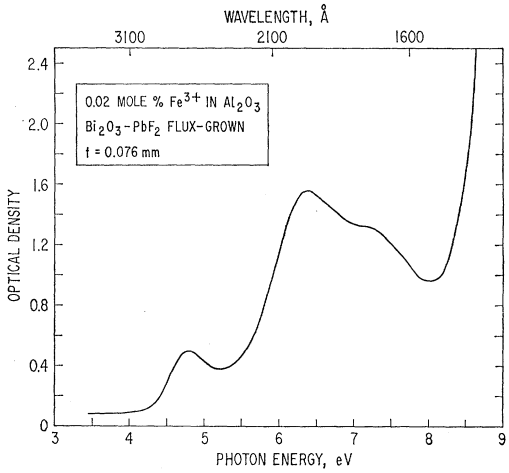

FIG. 9. Absorption spectrum of Fe^{3+} in Al_2O_3. At least three charge-transfer peaks are resolved.

samples is almost exactly offset by the thickness difference, so that the two spectra should be comparable. On the basis of the amount of Mg^{2+} and other unintentionally present ions reported in the spectrochemical analysis, it is believed that much of the Mn in the flux-grown sample is trivalent. This could explain the additional peaks observed for the flux-grown sample. The peak at 5 eV agrees well in the two cases, and the 6 eV peak of the Verneuil sample seems to correspond to the low-energy side of the composite peak near the same energy for the flux-grown sample.

The spectrum of Fe^{3+} is shown in Fig. 9. Fe^{3+} has the electron configuration d^5, which becomes $t_{2g}{}^3e_g{}^2$ in the octahedral crystal field and gives rise to a $^6A_1$ ground state. Since this is the only sextet state, all internal crystal-field transitions are spin-forbidden and hence extremely weak. At least three distinct charge-transfer peaks can be distinguished before the onset of the intrinsic edge. The lowest-energy peak corresponds to adding a spin-down electron to t_{2g}. In general, additional peaks could arise from any of several possibilities. For example, if the threshold transition is to t_{2g}, as is the case for Fe^{3+}, an additional peak should result for transfer to the higher-lying e_g orbital. Additional higher-energy peaks should also result if transfer occurs from a lower initial state on the oxygen to the same excited state on the metal ion. There is also the possibility that the transfer will originate from an oxygen ion more distant than the first nearest neighbor of the transition-metal ion. This would change the term analogous to the exciton binding energy term such that the total transition energy would be increased and would be analogous to transitions to the second exciton level for intrinsic absorption. An estimate of the energy difference to be expected for this latter case was considerably greater than for any of the observed peak separations, which tends to rule out this possibility.

The spectrum of Ni^{3+} is shown in Fig. 10. A factor-of-2 change in the vertical scale occurs at approximately 6 eV, so that the low-energy transitions can more easily be seen. The peak near 3 eV was observed by McClure[3] in exactly the same energy position and tentatively attributed by him to charge transfer because of its intensity. This is now seen to be the first of several intense bands, all of which are undoubtedly charge-transfer transitions. Note that this crystal is very dilute. However, even at this low concentration the sample has a pronounced yellow color. It therefore seems that Ni^{3+} is an example of visible charge transfer; that is, the low-energy tail of the 3-eV charge transfer extending down into the visible gives Al_2O_3 containing Ni^{3+} its well-known yellow color. This was the only case studied in which the charge transfer could be observed visually.

The absorption shoulder of pure Al_2O_3 at room temperature is shown in Fig. 11. The data in this case have been corrected for multiple internal reflections, so that within the experimental accuracy the curve represents the absolute absorption constant K versus photon energy. K was computed from solution of the equation

$$T=(1-R)^2e^{-Kt}/(1-R^2e^{-2Kt}), \qquad (7)$$

where T is the measured sample transmission, t the sample thickness, and R the reflectivity. For R, the reflectivity data of Arakawa and Williams[19] were used. The individual points computed are shown because of the considerable scatter of the data. This scatter is probably mostly due to charge transfer to residual trace impurities. The data were obtained from a flux-grown sample only 25 μ thick with a cross section of a few square millimeters. It was desirable to use as thin a crystal as possible so that measurements could be obtained for large absorption coefficients. Unfortunately, the thin samples had very small cross sections, which added to the difficulty of the measurements and hence the scatter of the data. It is believed that Fig. 11 represents the first measurements on bulk single crystals to such large values of K. From these measurements the position of the first exciton peak is estimated to be approximately 8.8 eV. This result is in agreement (within a few tenths of an eV) with earlier estimates made by Loh[20] and by Lemonnier *et al.*[21] from reflectance measurements and by Arakawa,[19] who used both single-crystal reflectance data and absorption data for thin anodized Al_2O_3 films.

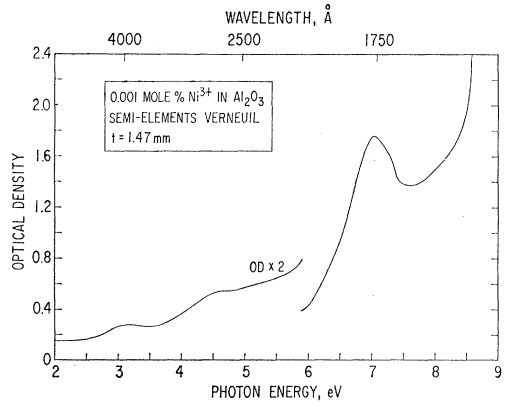

FIG. 10. Absorption spectrum of Ni^{3+} in Al_2O_3. The low-energy tail of the band peaked at 3.2 eV extends into the visible and gives the crystal a pronounced yellow color, even for very low Ni concentration.

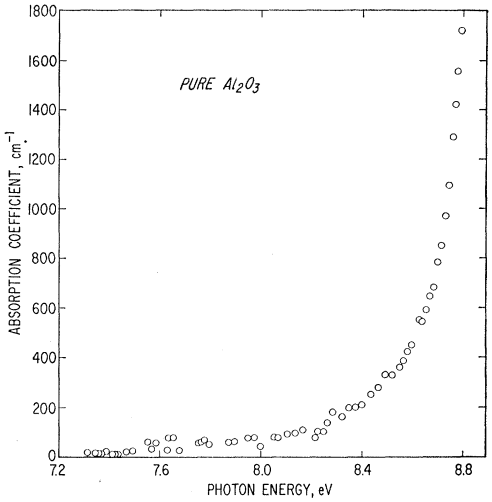

FIG. 11. Absorption coefficient of pure Al_2O_3. Within the experimental accuracy, the data are corrected for multiple internal reflections and are therefore absolute.

Several crystals containing the ions of Zr, Ru, Pd, or Ag of the 4*d*-transition series were examined for a uv spectrum. In each of these cases only a broad, structureless shoulder on the low-energy side of the intrinsic absorption was observed. This result prevented any quantitative comparison of the energy threshold, and for that reason the spectra will not be reproduced here. Another case studied, which was hoped to be especially interesting, was Ga^{3+}. The lowest unfilled level for Ga^{3+} is 4*s*, as compared to 3*s* for Al^{3+}. Since $I(Ga^{2+}) > I(Al^{2+})$ by 2.3 eV, it was, therefore, expected that Ga^{3+} would produce a spectrum on the low-energy side of the fundamental absorption. This was indeed the case, but again the spectrum was very broad and amounted to simply a pronounced shoulder on the low-energy side of the fundamental. In fact, the spectrum was almost identical to that of Ti^{3+} and will not be reproduced here. The large breadth of the 4*d*-series ions and Ga^{3+} absorption are consistent with the broadening mechanism to be discussed below.

[19] E. T. Arakawa and M. W. Williams, J. Phys. Chem. Solids **29**, 735 (1968).

[20] E. Loh, Solid State Commun. **2**, 269 (1964).

[21] J. Lemonnier, G. Stephan, and S. Robin, Compt. Rend. **262**, 355 (1966).

V. CONCLUSIONS

Table I summarizes the results for all of the ions studied. The observed peak positions are compared with the position of the threshold peak computed from Eq. (4). The constant energy term C in Eq. (4) is a simple average of the C's required to fit Eq. (4) to the threshold peak for the ions V^{3+}, Cr^{3+}, and Fe^{3+}. These three ions were chosen because they gave the best resolved spectra and provided a more reliable interpretation of results than did the other three ions. The value of $C=36.24$ eV, so determined, was then used to predict the position of the first peak for all the trivalent ions studied, as well as the edge position for intrinsic absorption. These calculated values are listed in column 5 adjacent to the experimental peak positions in column 4. The term ΔE_d is $-4\,Dq$ if the transferred electron enters a t_{2g} orbital (e.g., V^{3+}) and is $+6\,Dq$ if the electron must enter the higher-lying e_g orbital because the t_{2g} levels are filled (e.g., Cr^{3+}). The value of Dq used here was that of the trivalent ion, as tabulated by McClure.[3] A better value for ΔE_d would use a Dq for the initial state for the trivalent ion and for the final state for the divalent ion with allowance for the further reduction of Dq caused by the reduction of the final-state ligand charge. However, values for Dq for the divalent ion were not readily available, and it was felt that these corrections would not be large (especially between various members of the $3d$ series). The additional labor for this refinement, therefore, did not seem justified, especially in view of the many approximations already made. For the case of Ni^{3+}, an additional correction was included in the calculation of the threshold energy. This correction amounts to $-17.5B$ and is required because the ground state of Ni^{3+} in the crystal has the strong crystal-field configuration. The value of $10\,Dq$ for Ni^{3+} was not available in the literature and was therefore estimated as follows: Ni^{3+} is known to have the strong crystal-field configuration.[4] On the basis of the Dq/B values for the other members of the $3d$ series, it was assumed that Ni^{3+} is very near the ground-state crossover of the Sugano-Tanabe diagram. The $Dq/B=2.2$ at the crossover point together with the B value of 1115 cm^{-1} given by Tanabe and Sugano was then used to calculate Dq.

TABLE I. Summary of data obtained from charge-transfer spectra and comparison with systematics predicted from Eq. (4) of text. All energies are expressed in eV.

Ion	Mole% of dopant	Configuration	Peak positions	$36.24 - I(M^{2+}) + \Delta E_d$	$I(M^{2+})$	$10\,Dq$
Ti^{3+}	0.003	t_{2g}	~6.9	7.82	27.47	2.36
V^{3+}	0.03	t_{2g}^2	5.75	6.06	29.31	2.17
Cr^{3+}	0.01	t_{2g}^3	6.94	6.64	30.95	2.25
Mn^{3+}	~0.01	$t_{2g}^3 e_g$	4.15(?)	4.00	33.69	2.42
Fe^{3+}	0.02	$t_{2g}^3 e_g^2$	4.78 6.38 7.2	4.78	30.64	2.05
Ni^{3+}	0.001	$t_{2g}^6 e_g$	3.16 4.6 7.04	0.48	35.16	3.04
Al^{3+}	100	···	Edge 8.8	7.8	28.44	···

The agreement between calculated values and experimental peak positions for the three ions V^{3+}, Cr^{3+}, and Fe^{3+} is good to about 5%. This agreement is significant, even though the constant C was derived from these three ions, since the one value works well for all three. The diffuse peak observed for Ti^{3+} near 6.9 eV is within 1 eV of the calculated value of 7.82 eV. The calculated value for Mn^{3+} is 4.0 eV. This result is consistent with the peak at approximately 4.2 eV shown by the flux-grown sample, which is believed to contain some Mn^{3+} in addition to the Mn^{4+}. This peak is, therefore, quite reasonably identified with the Mn^{3+} charge-transfer threshold. The value of 0.48 eV calculated for Ni^{3+} is in poor agreement with the measured value of about 3.2 eV. Some possible explanations of this large difference are discussed below. As a further check on the charge-transfer model, it is interesting to use Eq. (4) to calculate the intrinsic absorption threshold. The result of 7.8 eV is within 1 eV of the experimental value of 8.8 eV deduced from Fig. 11. Therefore, with the exception of Ni^{3+}, the position in energy of the first absorption peak for all the $3d$-series ions studied relative to one another and to the position of the intrinsic absorption edge of Al_2O_3 is in good agreement with the charge-transfer model described by Eq. (4). In fact, the agreement is far better than was originally expected at the outset of these studies. The difference in ionic radii for the various ions probably makes a significant contribution to the energy differences. Different ionic radii could affect the large electrostatic terms ϵ_+ and ϵ_- in the threshold energy and thus produce a contribution to that part of the threshold energy that is characteristic of the particular ion. Such corrections would be difficult to evaluate but could probably account for most of the existing 5 to 10% disagreement.

There are several factors that could contribute to the poor agreement in the case of Ni^{3+}. It differs from all the other ions studied in the following ways: the $3d$ shell is more than one-half full, the ground state is a strong crystal-field case (i.e., the electron configuration is dictated by the crystal field rather than by the Hund's-rule requirement of maximum spin multiplicity), and the ground state undergoes a strong Jahn-Teller distortion. The Jahn-Teller stabilization energy is approximately 0.1 to 0.3 eV,[22] and has the proper sign to improve the agreement, but the magnitude is only a small fraction of the existing discrepancy. It is also quite possible that the Ni^{2+} ionization potential used is in error. This ionization potential[10] is based on unpublished data and could be approximately 1 to 2 eV too high. At the present time the ionization potential

[22] U. Höchli and K. A. Müller, Phys. Rev. Letters 12, 730 (1964).

seems to be the single most likely source of the disagreement.

The half-widths of the charge-transfer bands typically are 0.7 eV and independent of temperature. The mechanism responsible for such a large width is of interest, and some possible explanations are now considered. First, a width of about this magnitude would be expected from the same mechanism that broadens the crystal-field bands. The excited state on which the charge-transfer transition terminates is strongly coupled to the lattice, so the transition results in an excited vibrational state of the crystal. The absorption width therefore arises because of the different numbers of phonons excited in the absorption process. If one considers the configuration-coordinate diagram for the complex, the energy minimum of the excited electronic state is displaced from that of the ground state. Therefore, a vertical transition from one of the lower vibrational levels of the lower electronic state terminates on the sloping portion of the higher electronic state. Thus, there is a range of energies for which transitions can occur, and, because of the zero-point motion, this is true even for the lowest vibrational level. This broadening mechanism therefore exists even at 0°K and is consistent with the negligible temperature dependence observed for the bandwidths of the charge-transfer spectra. Although the previous mechanism is probably the dominant one, some contribution would also be expected from the broadening of the oxygen energy levels into a band in the crystal (valence band), as indicated in Fig. 2. It is difficult to estimate the magnitude of this contribution from the experimental results, but it must be less than or about equal to the vibronic contribution; otherwise, the absorption bandwidths would be even larger than those observed. It is also possible that the presence of the metal impurity ion could give an isolated cluster structure to the neighboring oxygen ion energy levels. In view of the strong covalency of the oxygen ions with the transition-metal ions as compared to the Al^{3+} ions this interpretation seems quite reasonable. This would effectively decouple the p levels of the neighboring oxygen ions from the p band so that the breadth of the p band would be irrelevant to the bandwidths of transitions between nearest neighbors.

The mechanism suggested above for the breadth of the charge-transfer bands is consistent with the much more diffuse Ti^{3+} absorption compared to the other ions studied. This is expected, since Ti^{3+} has the largest ionic radius of any of the $3d$-series ions. The radial extent of the $3d$ wave function, and hence the coupling of the $3d$ wave function to the lattice, should therefore be greater. This, in turn, should result in a broader absorption band. A similar argument would also apply to the cases of Ga^{3+} and the $4d$-series ions studied and would therefore explain their large breadth.

The data presented in Figs. 5–11 and summarized in Table I are consistent with the simple charge-transfer model described in Sec. II. It is believed that this result offers convincing support for use of the model in the qualitative interpretation of such spectra. Some experiments that should prove particularly useful in furthering the understanding of charge-transfer spectra are worthy of note. The study of oriented single crystals using polarized light will facilitate identification of the initial and final states involved in the transition. The excited electronic state would be expected to relax very quickly to the lowest vibrational state and thereafter proceed by radiative recombination, with a short lifetime, to the ground electronic state. A search for the recombination luminescence would be of interest, and if observed would provide important additional information about the charge-transfer excited state. A careful theoretical study of the charge-transfer problem in Al_2O_3 would be most welcome. It is hoped that the somewhat surprising success of the simple semiclassical charge-transfer model in predicting the threshold peak position will stimulate such studies. An important first step in such a study would be solution of the complete molecular orbital problem for the "free" complex MO_6 for all the $3d$-series ions.

ACKNOWLEDGMENTS

The author is indebted to Professor R. Orbach and Professor M. H. L. Pryce for stimulating discussions which were valuable in the interpretation of these experiments, to S. Duckett for helpful suggestions on certain aspects of the experimental problems, and to A. B. Chase and J. A. Osmer for providing the flux-grown samples. The valuable technical assistance of R. M. Mickels and W. Kalinowski, both in the performance of the experiments and in the reduction of the data, is sincerely appreciated.